

THE USE OF A LAMINAR FLAMELET APPROACH IN THE LARGE EDDY SIMULATION OF FLAME STRUCTURE AT THE BASE OF A POOL FIRE

by

Y. Kang and J.X. Wen
School of Engineering
Kingston University
Roehampton Vale, Friars Avenue
London, SW15 3DW
UNITED KINGDOM

and

K.B. McGrattan and H.R. Baum
Building and Fire Research Laboratory
National Institute of Standards and Technology
Gaithersburg, MD 20899, USA

Reprinted from the Interscience Communications Ltd.; Building Research Establishment; National Fire Protection Association; National Institute of Standards and Technology; Society of Fire Protection Engineers; and Swedish National Testing and Research Institute. Interflam '2001 .International Interflam Conference, 9th Proceedings. Volume 1. September 17-19,2001, Edinburgh, Scotland, Interscience Communications Ltd., London, England, 743-754 pp, 2001.

NOTE: This paper is a contribution of the National Institute of Standards and Technology and is not subject to copyright.



NIST

National Institute of Standards and Technology
Technology Administration, U.S. Department of Commerce

THE USE OF A LAMINAR FLAMELET APPROACH IN THE LARGE EDDY SIMULATION OF FLAME STRUCTURE AT THE BASE OF A POOL FIRE:

Y. KANG and J.X. WEN*

*School of Engineering, Kingston University
Roehampton Vale, Friars Avenue
London SW15 3 0W*

K.B. McGrattan and H.R. Baum

*National Institute of Standards and Technology
Gaithersburg, Maryland 20899-0001, U.S.A.*

* corresponding author

SUMMARY

A sub-grid scale combustion model, based on the laminar flamelet concept, has been implemented in the NIST LES based fire simulation code. It employs a conserved scalar, the so-called filtered mixture-fraction, to model the subgrid-scale (SGS) combustion. The SGS probability densityfunction of the mixture fraction is assumed to follow a beta-distribution. The local scalar dissipation rate is determined analytically by assuming that the mixing and reaction take place in local regions of steady, one-dimensional, laminar counterflow. The Smagorinsky model is used for the SGS turbulence closure. Predictions have been made for the methanol pool fire, which was experimentally tested by Weckman and Strong". Comparison with the experimental data focuses on the flame structure at the base of the pool fire. Reasonably good agreement has been obtained for velocity and temperature distributions and their fluctuations. To assess the effect of the SGS combustion model, additional comparison has also been made with our earlier simulation where the fire was simply prescribed as an ensemble of thermal elements ejecting from the burning surface at an initial velocity determined from the mass loss rate. It is shown that the inclusion of the flamelet based combustion model has led to more realistic predictions of the combustion and air entrainment processes at the base of the pool fire.

LARGE EDDY SIMULATION OF FIRES

In recent years, large eddy simulation (LES) has become an increasingly useful tool for investigating turbulent flows^{1,2}. In LES, the large-scale quantities are directly resolved. The quantities at scales smaller than the filtering width are filtered out and modelled by subgrid-scale (SGS) models. For application to combustion problems, both SGS turbulence and combustion models are needed to close the filtered Navier-Stokes equations. As the energy and mass transfer in a fully developed turbulence is dominated by the large eddies and SGS quantities are more homogeneous and steady, SGS models are expected to be more universal and less restricted to the particular type of flows considered during their development. Accordingly, LES is expected to generate more reliable results with appropriate SGS closures for combustion and turbulence⁵.

The application of LES to fires is complicated by the fact that the underlying chemical reactions typically take place within diffusion zones that are too thin to be resolved by the LES computational mesh. A feasible way to study the distribution of reactants and products within each LES grid cell is to assume the fire as an ensemble of thin flames that are locally one-dimensional³. In addition to the conservation equations of mass, momentum and energy, additional equations need to be solved for mass fractions of all major chemical species. The filtered equation for the mass fraction of the i th specie, Y_i , can be written as follows:

$$\frac{\partial}{\partial t}(\overline{\rho Y_i}) + \frac{\partial(\overline{\rho Y_i u_i})}{\partial x_i} = \frac{\partial}{\partial x_i} \left((\overline{\rho D})_i \frac{\partial \overline{Y_i}}{\partial x_{ii}} \right) + \overline{\dot{w}_i} - \zeta_{ij} \quad (1)$$

where ρ is density, D the diffusion coefficient, u_i the i -direction component of velocity vector and \dot{w}_i is the reaction rate. Variables with overbars represent the large-scale quantities. Comparing to the original governing equation, there is one additional term ζ_{ij} on the **right** hand side of the filtered equation, representing the small-scale quantities.

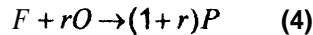
$$\zeta_{ij} = \frac{\partial}{\partial x_i} (\overline{\rho u_i Y_k} - \overline{\rho u_i} \overline{Y_k}) \quad (2)$$

To close equation (1) and give a theoretically accurate solution for Y_i , ζ_{ij} needs to be modelled. Similar to SGS turbulence modelling, the SGS mass transfer can be modelled as,

$$\overline{\rho u_i Y_k} - \overline{\rho u_i} \overline{Y_k} = -\overline{\rho} \frac{\mu_{ijk}}{Sc} \frac{\partial \overline{Y_k}}{\partial x_i} \quad (3)$$

In fires, the turbulent mixing time scale is larger than the chemical reaction time scale, which suggests a "quick" combustion. In those cases, the Damköhler number (defined as $Da = \tau_t / \tau_c$) is more than one.

The modelling of turbulent combustion has been conducted with both **equilibrium**³⁻⁵ and non-equilibrium **chemistry**⁶⁻⁹. The present study adopts the equilibrium approach proposed by Cook and Riley^{3,5}. It is based on the one-step, irreversible combustion,



where F , O and P represent fuel, oxidant and product, respectively. And r is the amount of oxidant that disappears upon reaction with a unit **mass** of fuel.

THE SGS LAMINAR FLAMELET COMBUSTION MODEL

The principle of the laminar flamelet based combustion model (LFM) LFM is to use a conserved scalar ξ , called mixture fraction, its variance, $\overline{\xi^2}$ and scalar dissipation rate χ to simulate filtered species concentration $\overline{Y_i}$ and reaction rate $\overline{\dot{w}_i}$, both need to be modelled.

The mixture fraction ξ and scalar dissipation rate χ are defined as following³,

$$\xi = \frac{Y_f - \frac{Y_o}{r} + \frac{Y_{o2}}{r}}{Y_{f1} + \frac{Y_{o2}}{r}} \quad (5)$$

$$\chi = \frac{\mu}{Pe} \nabla \xi \cdot \nabla \xi \quad (6)$$

Y_{f1} is the species concentration of fuel in the fuel stream and Y_{o2} is the species concentration of oxidizer in the oxidant stream. Equations (5)-(6) are based on two-feed non-premixed combustion with single fuel described by equation (4). The thin flame (laminar flamelet) is located in the vicinity of the stoichiometric surface, defined by **Cook''**,

$$\xi_{st} = \frac{Y_{o2}}{rY_{f1} + Y_{o2}} \quad (7)$$

Assuming that the flame is locally steady, and that ξ is a monotonic function of the local coordinates normal to the flame, the governing equation for Y_i can be transformed from physical space to ξ space⁹. Combining with equation (5), equation (1) can be rewritten as,

$$\frac{\partial \overline{\rho \xi}}{\partial t} + \frac{\partial (\overline{\rho \xi u})}{\partial x_i} = \frac{1}{Re Sc} \frac{\partial}{\partial x_i} \left(\mu \frac{\partial \xi}{\partial x_i} \right) + \zeta_\xi \quad (8)$$

In order to close the above equation, a widely used model for ζ_ξ was suggested by Moin¹¹,

$$\zeta_\xi = \frac{\partial}{\partial x_i} (\overline{\rho \xi u} - \overline{\rho \xi u}) = \overline{\rho} \frac{\partial}{\partial x_i} \left(\frac{\mu_{ijk}}{Sc} \frac{\partial \xi_k}{\partial x_i} \right) \quad (9)$$

The laminar flamelet equations can be generated by combining equations (5) and (6),

$$\chi(\xi, t) \frac{d^2 Y_f}{d\xi^2} = \dot{w}_f \quad (10)$$

The boundary conditions are as follows:

$$Y_f(\xi, \chi_0) |_{\xi=0} = 0 \quad (11)$$

$$Y_f(\xi, \chi_0) |_{\xi=1} = Y_{f1} \quad (12)$$

The species concentration of the oxidant and product can be obtained by,

$$Y_o = Y_{o2}(1 - \xi) + r(Y_f - \xi Y_{f1}) \quad (13)$$

$$Y_p = (r+1)(\xi Y_{f1} - Y_f) \quad (14)$$

The filtered species concentration is given by¹⁰,

$$\overline{Y_f} = \int_0^1 Y_f(\xi, \overline{\chi_0}) P(\xi) d\xi \quad (15)$$

where $P(\xi)$ is the probability density function (PDF). A similar method is used to get \overline{w} .

In LFM, both $\overline{Y_i}$ and $\overline{w_i}$ are modelled through $\overline{\xi}$, $\overline{\xi^2}$ and $\overline{\chi}$. The solution procedure can be divided into two parts. Firstly, the LES programme is run to get $\overline{\xi}$, $\overline{\xi^2}$ and $\overline{\chi}$. Secondly, $\overline{Y_i}$ and $\overline{w_i}$ are calculated through their relations to $\overline{\xi}$, $\overline{\xi^2}$ and $\overline{\chi}$. To get the right relations between $\overline{\xi}$, $\overline{\xi^2}$, χ and $\overline{Y_i}$, \overline{w} , equation (9) needs to be solved by laminar flame calculation to construct a look-up table prior to running the LES calculation.

For pool fires, the Mach numbers are generally low. Applying a low Mach number approximation to the governing equations, the ideal gas equation becomes³,

$$p^{(0)} = \rho T \quad (16)$$

where $P^{(0)}$ is the first-order thermodynamic pressure, which is constant in space and time^{3,12}. The temperature can be expressed as a function of $\overline{Y_i}$ and $\overline{\xi^3}$,

$$T = \left[T_1 - T_2 + \frac{(\gamma-1)}{\gamma} \sum h_i \cdot (Y_{i1} - Y_{i2}) \right] \cdot \xi + T_2 - \frac{(\gamma-1)}{\gamma} \sum h_i \cdot (Y_{i2} - Y_i) \quad (17)$$

where T_1 , T_2 are ambient temperatures in the fuel and oxidant stream, respectively. h_i is the enthalpy of formation of the i_{th} species and γ is the specific heat ratio.

The procedure of constructing a look-up table in incompressible combustion can be summarised as,

- i. Choose values of $\overline{\xi}$, $\overline{\xi^2}$, $\overline{\chi}$ as inputs.
- ii. Calculate $F(\xi)$ and $P(\xi)$ using the following equations³,

$$F(\xi) = \exp \{ -2 [\text{erf}^{-1}(2\xi - 1)]^2 \} \quad (18)$$

$$P(\xi) = \frac{\xi^{a-1} (1-\xi)^{b-1}}{B(a,b)}, \quad a = \overline{\xi} \left[\frac{\overline{\xi}(1-\overline{\xi})}{\overline{\xi^2} - \overline{\xi}^2} - 1 \right], \quad b = \frac{a}{\overline{\xi}} - a, \quad \overline{\xi^2} = \overline{\xi^2} - \overline{\xi}^2 \quad (19)$$

$B(a,b)$ is the Beta function.

- iii. As the local peak of χ can be expressed as¹⁰,

$$\chi = \overline{\chi_0} F(\xi) \quad (20)$$

The filtered value of the local peak of χ within the layer χ_0 ($\chi_{0\min} \leq \chi_0 \leq \chi_{0\max}$) is obtained by¹⁰

$$\bar{\chi}_0 = \frac{\bar{\chi}}{\int_0^1 F(\xi) P(\xi) d\xi} \quad (21)$$

iv. After replacing χ by $\bar{\chi}_0 F(\xi)$ in equation (10), and using the boundary conditions in equations (11) and (12) to get $Y_i(\xi, \bar{\chi}_0)$, the reaction rate in equation (10) is initialised with the Arrhenius expression^{13,20,21}

$$\bar{w} = A \bar{\rho}^2 \bar{Y}_i \bar{Y}_j T^b \exp\left(-\frac{E}{RT}\right) \quad (22)$$

v. Insert LFM solution $Y_i(\xi, \bar{\xi}^2, \bar{\chi})$ into equation (16) to get the temperature

vi. Use equation (16) to get density.

vii. With ρ and $P(\xi)$ known, a Favre-filtered process is applied to re-calculate $\bar{\xi}, \bar{\xi}^2$,

$$\bar{\xi} = \frac{\int_0^1 \rho \cdot \bar{\xi} \cdot P(\xi) d\xi}{\int_0^1 \rho \cdot P(\xi) d\xi} \quad (23)$$

$$\bar{\xi}^2 = \frac{\int_0^1 \rho \cdot \bar{\xi}^2 \cdot P(\xi) d\xi}{\int_0^1 \rho \cdot P(\xi) d\xi} \quad (24)$$

viii. Repeat steps I-IV using the updated $\bar{\xi}$ and $\bar{\xi}^2$ to get the tabulated value $Y_i(\bar{\xi}, \bar{\xi}^2, \bar{\chi})$

ix. Use equation (15) to get filtered value

x. Construct the look-up table by repeat steps I-V for the full range of $\bar{\xi}, \bar{\xi}^2, \bar{\chi}$ as expected by LES.

EXPERIMENT CONSIDERED

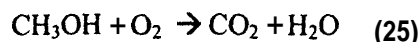
The pool fire experiment of Weckman and Strong¹⁴ was set on a circular burner with a diameter of 30.5 cm. Methanol was feed at a constant rate of 1.35 cm³/s to give a total heat release rate of 24.6 KW. The ambient temperature was 15°C at the beginning of the simulation. The experiments covered all three distinctive regions of pool fires, i.e. the "persistent flame region" ($Z/Q^{2/5} < 0.08$), the "intermittent flame region" ($0.08 < Z/Q^{2/5} < 0.2$) and the "fire plume" region ($Z/Q^{2/5} > 0.2$). However, only details of the data for the persistent flame region and the lower part of the intermittent flame region were given in the paper. Also the reported experimental data was restricted to the fire region

within a radius of 16 cm, i.e. just slightly over the edge of the methanol pool with a radius of 15.25 cm. Accordingly, the discussion in the paper will be limited to this region as well. Because of the very rapid chemical reaction and air entrainment, this is the most critical region concerning the establishment of the pool fire and the most challenging region for numerical simulations.

COMPUTATIONAL DETAILS

The computational domain is 1.28m(W) X 1.28m(D) X 2.56 (H). Several grid sizes have been tested but no significant improvement has been found in the results when the resolution is finer than 64 X 64 X 128. As such, this has been chosen as the final mesh resolution. The grids representing the burner area have been further stretched to give a cell dimension less than 1 cm. The simulation was carried out on a Compaq XP1000 Unix Workstation, with 512M RAM and 9G Hard Disc. One complete simulation takes about 70 hours. The instantaneous data from LES are found to appear in regular cycles after marching sufficient time. The mean values for temperature and velocity distributions are obtained by averaging the values in the latest cycle. Their fluctuations are calculated as the deviation of instantaneous values from the mean.

The LFM has been implemented into the NIST LES code¹⁵ used to carry out the calculation. The following one-step, irreversible reaction is assumed for the open-air combustion of the pool fire,



The corresponding value of r in equation (4) is 1.5.

The Smagorinsky model¹⁶ was used for SGS turbulence modelling. The relaxation method of Fox¹⁷ has been adopted to solve the two-point boundary differential equation (10). After the look-up table has been constructed, the species concentration of methanol in each cell can be obtained according to the mixture fraction calculated from the LES calculation. The mass fractions of the grid-scale oxidant and product can then be computed by equations (13) and (14). The mixture fraction and mass fractions of reactants and products are put into equation (17) to get the temperature. The density is calculated by equation (16). The updated temperature and density are then feed back into the LES calculation for a new iteration.

Circular pool fires have been assumed to be axis-symmetric in most simulations to save computational time. Reasonably good results of helium and methanol fires have been found by some within a limited height¹⁸. However, as experimentally observed by Mell et al.²², pool fires are not truly axis-symmetric. In the current 3-D simulation, the deviation from an axis-symmetric distribution is clearly observed and the simulation generates reasonably good results as compared to the experimental data.

ANALYSIS OF SIMULATION RESULTS

Mean temperature and axial velocity throughout the fire domain are analysed and compared with the experiment data¹⁴. The radial velocity is presented to examine the air entrainment from the side. This was significantly over-predicted in our previous simulation where the fire was simply prescribed as an ensemble of thermal element ejecting from the pool surface¹⁹. Apart from the mean quantities, the root mean square (rms) values of temperature T' defined

as $T' = \sqrt{\frac{\sum T'^2}{n}}$, is also shown on a contour. Some results from our previous simulation¹⁹ are presented as well to highlight the improvement achieved by the use of the LFM SGS combustion model.

Mixture Fraction

As the combustion process is mainly determined by the mixing of large eddies, the mixture fraction, defined by equation (5), plays an important role in the prediction of temperature and velocity distribution. Fig. 1 shows the evolution of mixture fractions at different heights.

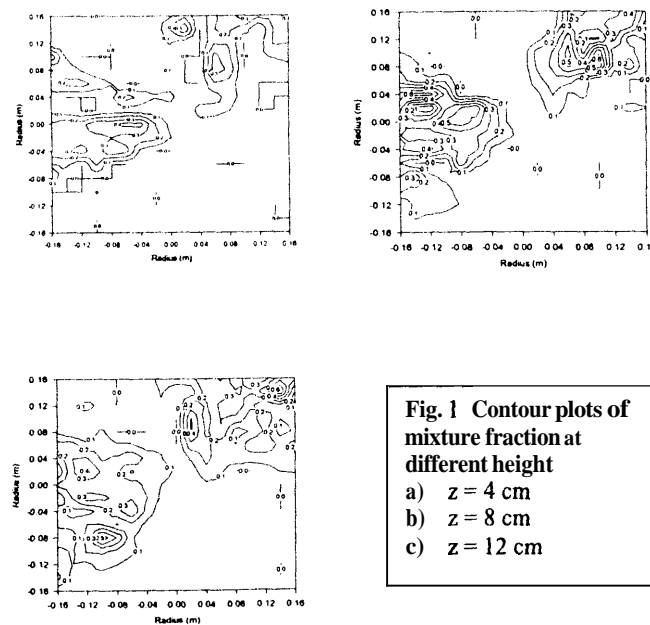


Fig. 1 Contour plots of mixture fraction at different height

- a) z = 4 cm
- b) z = 8 cm
- c) z = 12 cm

It is seen that the fuel and oxidant start mixing at the rim of the burner near the fuel surface. More air is entrained from outside with the increase in height. As defined by equation (7), the stoichiometric surface is located at $\xi = 0.4$, where the fuel and oxidant are in exact stoichiometric proportion and the combustion has the highest efficiency. The mixture fraction starts to decrease at a height above 12 cm because more products are generated and more reactant consumed.

Mean temperature

Fig. 2 is a contour plot of the mean temperature. The highest temperature occurs at the centreline and decreases with the height. The temperature also decreases along the radius. From 4cm above the fuel and 6cm from the centreline of the fire, the mean temperatures remain less than 1200K, which agrees well with the experimental data.

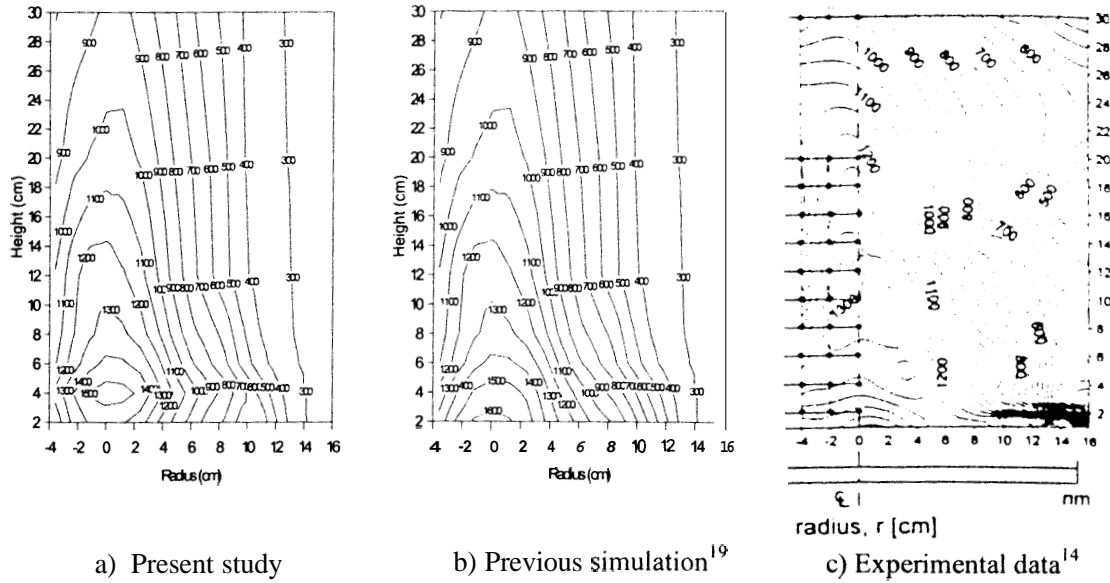


Fig. 2 Isotherm of mean temperature from LFM simulation

As seen from the line plots in Fig. 3, the predictions and experimental data both have the same distribution of temperature throughout the fire domain. The highest temperature occurs along the centreline. At 4 cm above the pool surface, both the present predictions and our previous results over-predict the temperature at the centreline. This over-prediction is gradually reduced with the increase in height. In general, the present prediction with the LFM SGS combustion model, is closer to the measured data than our previous simulation with the

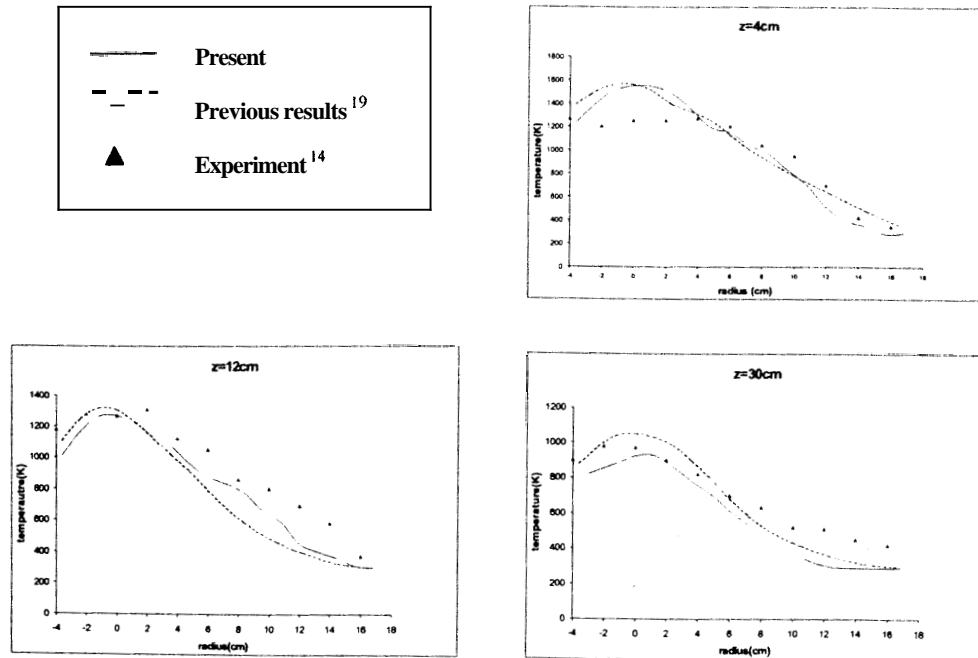


Fig. 3 Mean temperature at different heights

Axial and Radial Velocity

Similar to the distribution of temperature, the highest axial velocity is located along the centreline, representing the rapid mixing of reactants due to combustion and convection. The peak value increases with the height as the flow is continuously accelerated by combustion generated buoyancy. The axial velocities decrease along the radius with the reduction of combustion intensity away from the centre core region. Both the present and previous predictions are in good agreement with the experimental data at the area more than 6 cm from the centreline. But they over-predict the axial velocities in the core region surrounding the centreline. As there are many uncertainties associated with the transient combustion processes and the transition from laminar to turbulent flow at the base of the pool fire, it is likely that the present modelling approach, although offering some improvement, has still not fully captured the dynamics of this region. With the gradual increase in height, the influence of turbulent mixing overtakes that of chemical reaction, the predictions are in better agreement with the data.

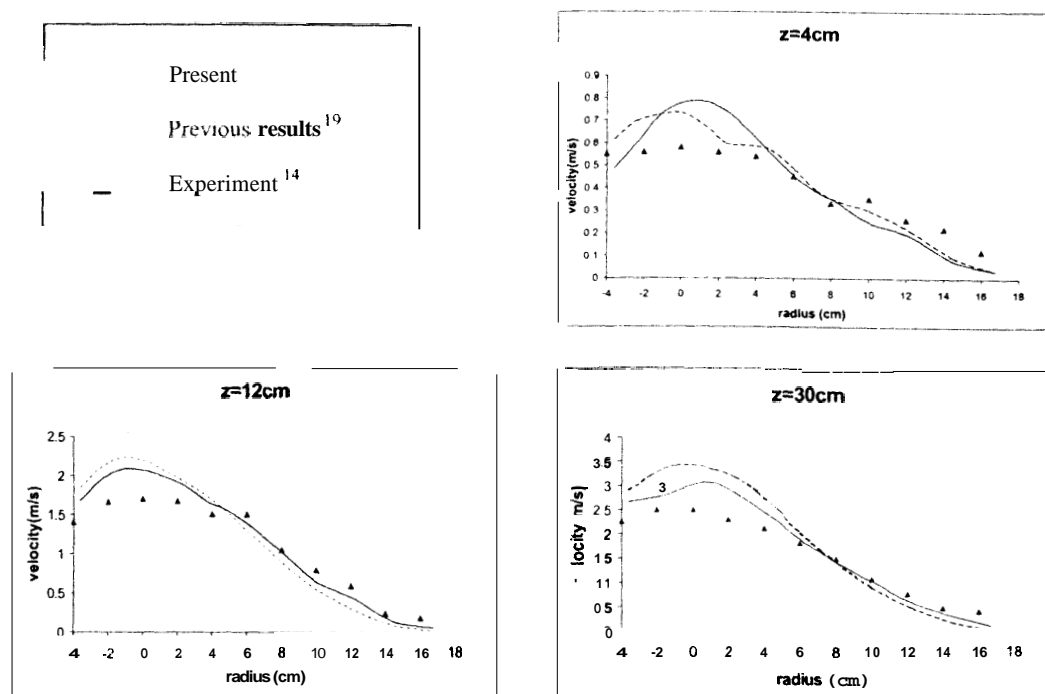


Fig. 4 Mean axial velocities at different height

The radial velocity represents the air entrainment. This was significantly over-predicted in our previous simulation with the simplified treatment for combustion¹⁹. With the use of LFM, the improved simulation of the SGS combustion processes have led to more accurate predictions of the air entrainment. The contour plots of mean radial velocities are shown in Fig. 5. A strong radial inflow of ambient air (approximately 0.35 m/s) occurs at radial positions of between 12 and 16 cm at 2 cm above the pool surface. This agrees well with the measurement by Weckman and Strong¹⁴. Another strong entrainment region can be seen within radial positions between 8 cm to 12 cm at 8 cm to 12 cm above the burner surface. At the height of 20 cm above the pool surface, the magnitudes of the radial velocities are significantly less due to the anticipated reduction in air entrainment. The detailed comparison between the present

prediction and the experimental data at three heights is shown in Fig. 6. Generally, there are still some discrepancies which call for further tuning of the SGS closure.

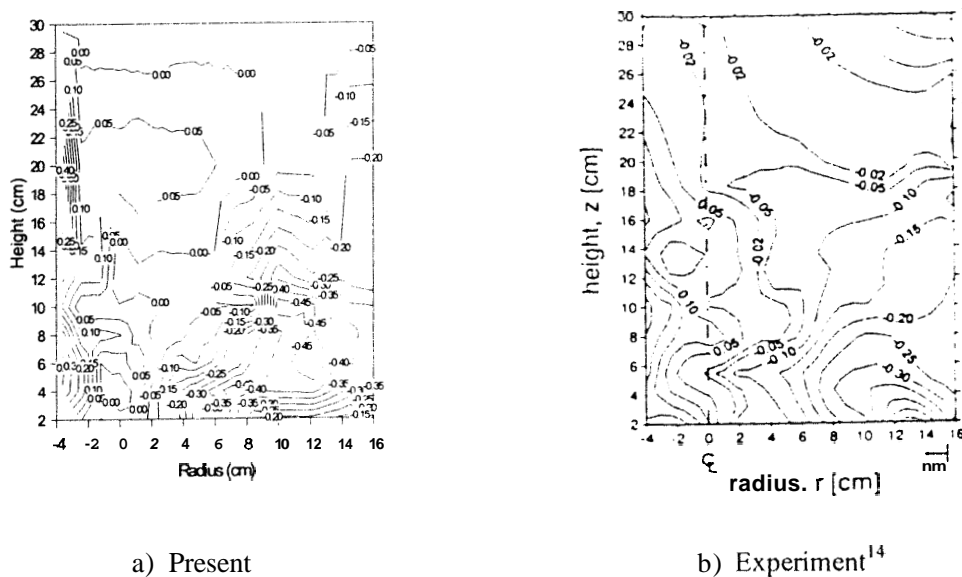


Fig. 5 Isovels of mean radial velocity (m/s)

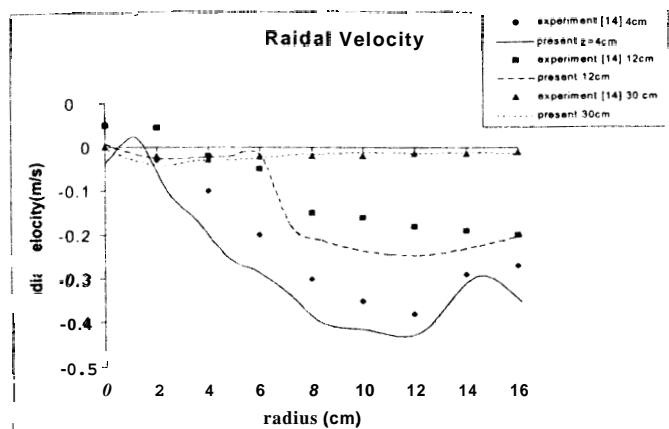


Fig. 6 Mean radial velocities at different heights (m/s)

Root Mean Square (rms) temperature

The distribution of rms temperature is shown in Fig. 6. The highest values are located near the burner rim, at radial positions between 8 to 12 cm. In addition, there are relatively high rms values near the centreline at heights lower than 8 cm, which shows the uncertainties in the transient area. As shown by the line plots for different heights in Fig. 8, the rms temperature decreases gradually with height and from the centreline to the outside area. Again better agreement has been achieved in the outer region than near the centre.

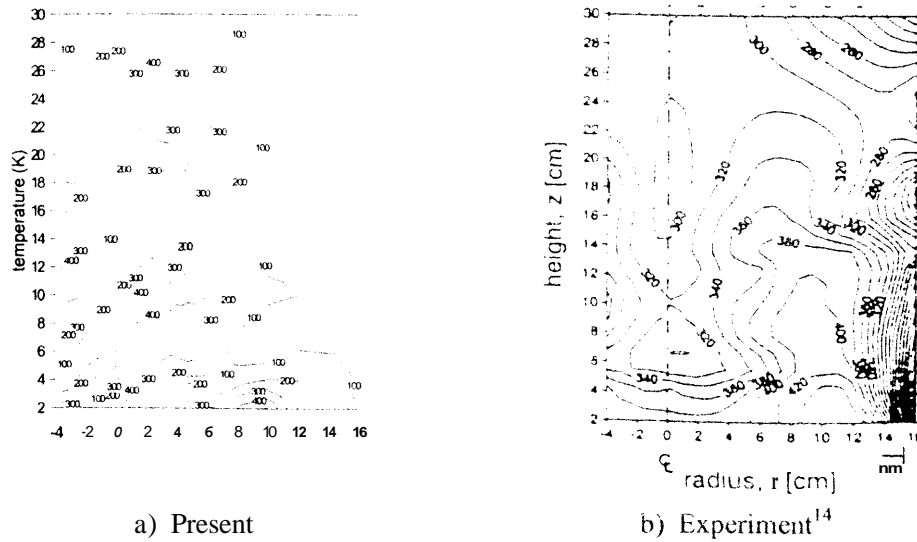


Fig. 7 Contour plot of rms temperature distribution (K)

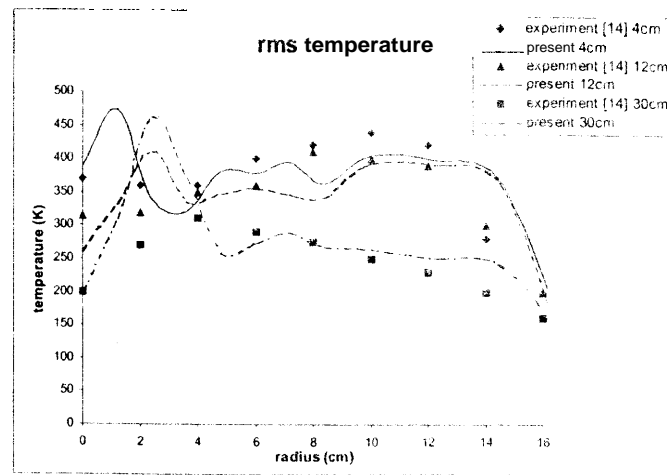


Fig. 8 rms temperature at different heights (K)

CONCLUSION

A laminar flamelet model (LFM) is used for SGS combustion closure in large eddy simulation (LES) to analyse the turbulence structure of a medium-scale methanol pool fire. A separate one dimensional laminar flame code has been written to generate the **look-up** table which relates the species concentration to the mixture fraction, its variance and the scalar dissipation rate. After the mixture fraction is calculated by an additional transport equation in the LES calculation, the mass fraction of reactants and products are obtained from the **look-up** table through a prescribed PDF approach. The predictions have been compared with the pool fire data of Wechman and Strong¹⁴ and our previously published results¹¹ where the fire was prescribed as an ensemble of thermal elements ejecting from the burning surface. Reasonably

good agreement has been found between the predicted and measured mean temperature and axial velocity distributions. In comparison with our earlier results¹⁹, much more realistic predictions have been obtained for air entrainment at the base of the pool fire and this has led to better agreement between the predicted and measured radial velocities. The predicted rms temperature values are also closer to the experimental data implying that the temperature fluctuations have been reasonably predicted. While the use of the LFM has offered some improvement over simplified treatment for combustion, the current model has still not fully captured the dynamics at the base of the pool fire. Work is underway to further tune the LFM model and couple it with Germano's²³ dynamic approach for SGS turbulence closure. Further validation with fresh experimental data will also be carried out.

REFERENCES

1. Rodi, W., Ferziger, J.H., Breuer, M. and Pourquie, M., *Transactions of the ASME*, Vol. 119, pp.248-262 (1997)
2. Kerstein, A.R., *J. Fluid Mech.*, vol. 216, pp.411-435(1990)
3. Cook, A.W. and Riley, J.J., *COMBUSTION AND FLAME* 112:593-606 (1998)
4. Frankel, S.H., Adumitroaie, V., Madnia, C.K. and Giv, P., *Fluids Engineering Division, ASME*, 1993, vol.162, pp.81-101
5. Cook, A.W. and Riley, J.J., *Phys. Fluids A* 6:2868-2870(1994)
6. Bilger, R.W., *Topics in Applied Physics, Springer-Verlag, Berlin*, 1980, vol.44, ch. 3
7. Lentini, D., *Comb. Sci. Tech.*, 1994, vol.100, pp. 95-122
8. Pope, S.B., *Phil. Trans. R. Soc. London*, 1979, Vol. 291, pp. 529-568
9. Peters, N., *Prog. Energy Comb. Sci.* 1984, vol. 10, pp. 319-339
10. Cook, A.W., Riley, J.J. and Kosaly, G., *COMBUSTION AND FLAME* 109:332-341(1997)
11. Moin, P., Squires, K., Cabot, W. and Lee, S., *Phys. Fluids A* 3:2746-2757 (1991)
12. Cook, A.W. and Riley, J.J., *J. Comput. Phys.* 129:263-283 (1996)
13. Veynante, D. and Poinsot, T., *TURBULENT COMBUSTION*, pp. 105-140, 1998
14. Weckman, E.J. and Strong, A.B., *COMBUSTION AND FLAME* 105:245-266(1996)
15. McGrattan, K.B., Baum, H.R., Rehm, R.G., Hamins, A. and Forney, G.P., *Fire Dynamics Simulator – Technical Reference Guide*, NISTIR 6467, January 2000, National Institute of Standards and Technology, U.S.A.
16. Smagorinsky, J., General circulation experiments with the primitive equations, *Part I. The basic experiment*, Monthly weather review, pp.91, 99-152, 1963.
17. Fox, L., *The numerical solution of two-point boundary problems in ordinary differential equations*, 1957, The Clarendon Press, Oxford.
18. Mell, W.E., McGrattan, K.B. and Baum, H.R., *Twenty-sixth Symposium (international) on Combustion*, Vol. 1, pp. 1523-1530(1996)
19. Kang, Y., Wen, J.X., Lo, S., McGrattan, K.B. and Baum, H.R., *Large Eddy Simulation of A Medium Scale Methanol Pool Fire*, Proceedings of the 3rd International Seminar on Fire and Explosion Hazard, Lake District, England, 10th-14th, 2000.
20. Cox, G. and Chitty, R., *Fire and Materials*, Vol. 6, NOS 3 and 4, pp. 127-134, 1982
21. Turns, S.R., *An Introduction to Combustion Concepts And Applications*, Propulsion Engineering Research Centre and Department of Mechanical Engineering, The Pennsylvania State University, McGraw-Hill Inc. , 1996.
22. Mell WE, McGrattan KB and Baum HR, Johnson SW and Pitts WM, Fall 1995 Western States Section meeting/Combustion Institute, Stanford, CA, <http://odie.seas.ucla.edu/WSS/papers/fp5f22.html>.
23. Germano M, Piomelli U, Moin P and Cabot WH, A dynamic subgrid scale eddy viscosity model, *Physics of Fluids*, A3(7), 1991.